

## TiO<sub>2</sub>/ZnO: TYPE-II HETEROSTRUCTURES FOR ELECTROCHEMICAL CRYSTAL VIOLET DYE DEGRADATION STUDIES

Dilip Kumar Behara\*, Jalajakshi Tammineni, Mukkara Sudha Maheswari

Department of Chemical Engineering, JNTUA College of Engineering, Ananthapuramu-515002,  
Andhra Pradesh, India  
dileepbh.chemengg@jntua.ac.in

Semiconductor nanomaterials with proper band edge alignments forming “heterostructure” assemblies have significant importance in water splitting, dye degradation, and other electrochemical studies. The formed heterojunction between material phases facilitates fast charge carrier transport and, thereby, improves electrochemical performance in associated processes. Herein, we report a type-II heterostructure combining TiO<sub>2</sub> and ZnO nanomaterials for electrochemical crystal violet dye degradation studies. The rationale in choosing the above materials (TiO<sub>2</sub>, ZnO) in the present study includes stability, lack of toxicity, and high oxidation power, but they also facilitate fast charge carrier movements due to proper band edge alignments, forming a type-II heterostructure assembly. Cyclic voltammetry, combined with ultraviolet-visible analysis, was used to identify the cathodic and anodic peak currents and trace the exact mechanism of dye degradation. The electro-catalytic performance of TiO<sub>2</sub>/ZnO heterostructured materials fabricated on titania (Ti) substrate show higher performance, in comparison to all individual material interfaces, due to synergistic interaction and synchronized charge transport.

**Keywords:** TiO<sub>2</sub>; ZnO; type-II heterostructure; electrochemical; dye degradation

## TiO<sub>2</sub>/ZnO: ХЕТРОСТРУКТУРИ ОД ТИПОТ-II ЗА ПРОУЧУВАЊЕ НА ЕЛЕКТРОХЕМИСКО ДЕГРАДИРАЊЕ НА КРИСТАЛНО ВИОЛЕТОВА БОЈА

Полупроводливите материјали со соодветно израмнување на рабовите на лентите што образуваат „хетероструктурен“ склоп имаат значајна важност во разложување на водата, на боите и во други електрохемиски проучувања. Образованата хетероврска меѓу фазите на материјалот го олеснува брзиот пренос на полнежот и соодветно ги подобрува електрохемиските карактеристики на придружните процеси. Во овој труд ја објавуваме хетроструктурата од типот-II добиена со комбинација на наноматеријали од TiO<sub>2</sub> и ZnO за испитување на електрохемиско разложување на кристално виолетовата боја. Мотивот за изборот на наведените материјали (TiO<sub>2</sub>, ZnO) во оваа студија се стабилноста, отсуството на токсичност и високата оксидациона способност, но исто така и тоа што тие го олеснуваат брзиот пренос на полнеж, што се должи на правилното рамнување на рабовите на лентите што го образуваат хетероструктурниот склоп од типот-II. Идентификацијата на катодните и анодните пикови на струјата и следењето на точниот механизам на разложувањето на бојата беше извршено со примената на циклична волтаметрија комбинирана со ултравиолетова видлива анализа. Електрокаталитичкото однесување на хетероструктурниот материјал на TiO<sub>2</sub>/ZnO нанесен на субстрат од титан покажува подобри перформанси во споредба со сите индивидуални интерференции на материјалите, што се должи на синергетската интеракција и синхронизираните пренос на полнеж.

**Клучни зборови:** TiO<sub>2</sub>; ZnO; тип-II хетероструктура; електрохемиски; разложување на бои

## 1. INTRODUCTION

Synthetic dyes are widely used in numerous fields, such as the textile industry [1, 2], the leather industry [3], food technology [4], light harvesting arrays [5] and photo-electrochemical cells [6]. Release of these synthetic dyes without prior treatment in water bodies affects aquatic life by blocking sunlight, as well as reducing the re-oxygenating nature of water. Therefore, treating streams containing dyes before they let into water bodies is imperative. Several dye degradation routes, such as physical, chemical, and biological, persist and are effective in treating dye effluents. However, each method has its limitations. For example, in the case of chemical methods, chemical coagulation creates waste dumping problems, addition of new chemicals, and low concentration ranges [7], whereas reverse osmosis and ultra-filtration are quite expensive. Similarly, formation of sludge and regeneration of the absorbents are two main obstacles in physical methods. Lastly, the high molecular mass of dyes makes biological methods ineffective [8]. Recently, processes, such as ozonation [9] and photo-oxidation [10, 11], have been proposed as alternative methods, but they are limited by the high cost. Therefore, developing cost-effective alternatives to conventional approaches is essential.

In contemporary research, electrochemical techniques were found to be better alternative methods in treating dye effluents in a more environmentally friendly and economic way. These methods are effective in removing dyes from water with the aid of anode materials (electro-catalysts) having good electrochemical stability in strong destructive media. These methods have special properties, such as simple equipment, easy operation, lower operating temperature, low-volume application, environmental compatibility, and a wide potential window, compared with other techniques [12–14]. Further, the process requires significantly less area, equipment and flexibility to operate under a wide variety of conditions, *i.e.* current density, different electrodes, different pH and different dye concentrations than the conventional treatment processes [15, 16].

Semiconductors/metal oxides as potential anode materials play an important role in mineralizing dyes and provide a percolation path for charge carrier movements inside the crystalline lattice. Several semiconductor nanomaterials, such as TiO<sub>2</sub>, ZnO, Fe<sub>2</sub>O<sub>3</sub>, CeO<sub>2</sub>, CdO, *etc.*, were reported for photoelectrochemical/electrochemical dye degradation studies [17–21]. However, using a combination of semiconductor materials in the form of composite assemblies or "heterostructures"

is advantageous, as they utilize synergistic interaction between material phases and extract better electric flux at the interface junctions than individual material assemblies. Further, proper band edge alignments facilitate charge carrier movements at a faster rate and improve the electrochemical performance of the process under consideration [22, 23]. Herein, we report a type-II heterostructure assembly combining TiO<sub>2</sub> and ZnO for crystal violet dye degradation studies. The rationale in choosing the above materials (TiO<sub>2</sub>, ZnO) in the present study includes stability, lack of toxicity, and high oxidation power, but they also facilitate fast charge carrier movements due to proper band edge alignments. Heterostructure formation is expected to improve the charge carrier transport path as well as catalytic performance by increasing electrochemical active surface area (ECSA) [24]. The fabricated electrodes were characterized using X-ray diffraction (XRD), scanning electron microscopy (SEM), energy dispersive X-ray spectroscopy (EDS), and Fourier transfer infrared spectroscopy (FTIR).

In the present study, cyclic voltammetry (CV) and ultraviolet-visible (UV-Vis) spectrometry was performed to examine the degradation efficiency of the crystal violet dye. The synthesized TiO<sub>2</sub>, ZnO, and TiO<sub>2</sub>/ZnO nanoparticle assemblies were fabricated as electrodes on titanium (Ti) and indium tin oxide (ITO) substrates and used as an anode in electrochemical analysis. The TiO<sub>2</sub>/ZnO heterostructure assembly fabricated on Ti substrate (TiO<sub>2</sub>/ZnO@Ti) showed complete decolorization within 6 h of electrochemical treatment compared to all other fabricated electrodes (composite, as well as individual materials). The degradation time to reach 80 % decolorization for bare Ti, Ti/ZnO, Ti/TiO<sub>2</sub>, and Ti/TiO<sub>2</sub>/ZnO was 12, 10.5, 9 and 6.5 h, respectively. The enhanced performance of the composite heterostructure assembly was ascribed to synchronized charge transport and synergistic interaction between the material interfaces. The results of this study not only help to understand the molecular degradation mechanism of complex dye molecules but also paves path towards design low cost materials for improved electrochemical performance.

## 2. MATERIALS AND METHODS

Zinc acetate di-hydrate [Zn(O<sub>2</sub>CCH<sub>3</sub>)<sub>2</sub>·(H<sub>2</sub>O)<sub>2</sub>], ethanol (C<sub>2</sub>H<sub>5</sub>OH), triethanolamine (C<sub>6</sub>H<sub>15</sub>NO<sub>3</sub>), Tii-so-propoxide [Ti{OCH(CH<sub>3</sub>)<sub>2</sub>}<sub>4</sub>], ammonia (NH<sub>3</sub>), sodium sulfate (Na<sub>2</sub>SO<sub>4</sub>), and isopropyl alcohol (C<sub>3</sub>H<sub>8</sub>O) were purchased from Sigma Aldrich Chemicals (India) Ltd. Nafion (10 %) liquid solution was purchased from Dupont Chemicals, USA.

Crystal violet dye was purchased from Sigma-Aldrich. All the reagents were analytically pure and used as received without further purification. Deionized water was used in the experiments.

### 2.1. Synthesis of TiO<sub>2</sub> nanoparticles

Ethanol (150 ml) and deionized water (3.75 ml) were added and stirred for half an hour, until

the formation of a homogenous solution. Nine ml of Titanium(IV)-Iso Propoxide (TTIP) was added, dropwise, into the homogeneous mixture. The reaction mixture was kept under agitation for 4 h at 85 °C under magnetic stirring. After that, the sample was dried at 60 °C for 30 min and calcined in a muffle furnace for 3 h at 400 °C to yield the anatase TiO<sub>2</sub> phase (Fig. 1) [24].

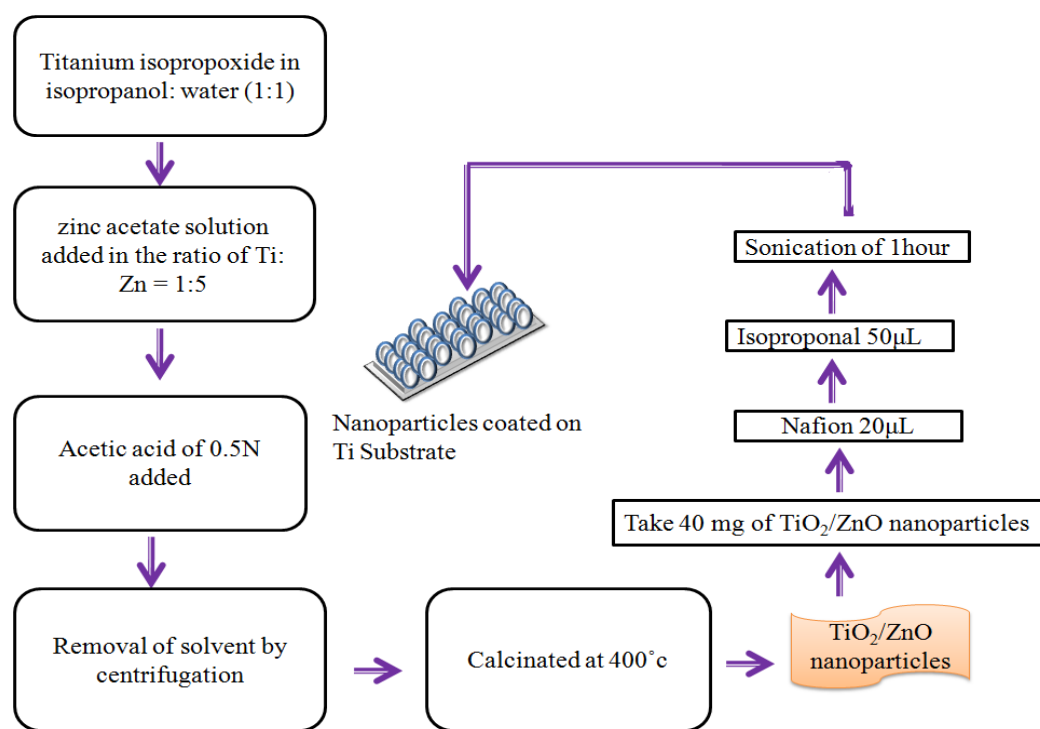


**Fig. 1.** Schematic representation of the synthesis and fabrication of nanoparticles on Ti substrate

### 2.2. Synthesis of ZnO nanoparticles

ZnO nanoparticles were prepared by a chemical reduction method. Thirty ml of triethanolamine (TEA) and 20ml of deionized water were mixed. Then, 2 ml of ethanol was added dropwise and stirred for 2 h. Then, 5.39 g of zinc acetate dihydrate was taken in a 50 ml of deionized water and stirred for 20 min. Next, 0.5 ml ethanol was added to the zinc acetate solution and stirred for ½ h. The particles were centrifuged, followed by drying at 95 °C in a hot air oven for 8 h, and finally, the sample was calcined for 3 h at 500 °C, as shown in Figure 1 [25].

### 2.3. Synthesis of TiO<sub>2</sub>/ZnO nanocomposites

TiO<sub>2</sub>/ZnO nanocomposites were synthesized via the sol-gel method. TTIP was taken in a 1:1 ratio of isopropanol and water. Zinc acetate was

added in the ratio of 1:5 Ti/Zn, along with 0.5N acetic acid. The sample was stirred overnight. The solvent was removed by centrifugation, and then, the sample was calcined at 400 °C for 4 h, yielding TiO<sub>2</sub>/ZnO nanocomposites, as shown in Fig. 1 [26].

### 2.4. Fabrication of electrode

Forty mg of nanoparticles (TiO<sub>2</sub>, ZnO, TiO<sub>2</sub>/ZnO) were mixed with 2 ml of isopropanol and 20 µl of Nafion. Then, the mixture was sonicated for 1 h; the slurry was applied on a Ti plate (effective electrode surface ~1 cm<sup>2</sup>) and dried at 60 °C on a hot plate.

### 2.5. Electrochemical analysis

CV experiments were carried out at room temperature using a potentiostat (K-lyte 1.0). The

cell used for voltammetric experiments was a three-electrode type with an Ag/AgCl reference electrode, Pt mesh counter electrode (Fig. S1, Supplementary Information), and Ti/TiO<sub>2</sub>, Ti/ZnO, or Ti/TiO<sub>2</sub>/ZnO as working electrodes with 0.1 M Na<sub>2</sub>SO<sub>4</sub> solution as the supporting electrolyte. Voltammetric studies were performed at fixed voltages of 0.6, 1.2, 1.3 and 1.0 V for bare Ti, Ti/TiO<sub>2</sub>, Ti/ZnO and Ti/TiO<sub>2</sub>/ZnO, respectively, at a scan rate of 0.05 V/s. These are the potentials where the oxidation peak hump begins. A dye concentration of 55 mg/l with 1M Na<sub>2</sub>SO<sub>4</sub> was used as supporting electrolyte solution for all electrochemical experiments.

A UV-Vis spectrophotometer was used to measure the decolorization efficiency at different time intervals and was calculated by the following formula [1]:

$$\% \text{ decolorization} = (A_0 - A) / A_0 \times 100, \quad (1)$$

where  $A_0$  and  $A$  are the absorbance (at the maximum wavelength,  $\lambda_{\text{max}}$ ) of dye solution before/initial (at  $t = 0$ ) and after electrochemical treatment (at  $t > 0$ ).

### 3. RESULTS AND DISCUSSION

#### 3.1. XRD analysis

To identify the crystalline structure of synthesized materials, XRD spectra/patterns were recorded (Fig. 2). The diffractogram patterns were indexed properly for all crystalline peaks and compared with the JCPDS data files. The major peaks at  $2\theta$  values of 25.5°, 40.0°, 48.0°, 54.2° and 62.4°, shown in Fig. 2a, correspond to the atomic planes (101), (004), (102), (110), and (211) of tetragonal anatase TiO<sub>2</sub> (JCPDS Card No. 21-1272), respectively [24]. The average crystallite size of the TiO<sub>2</sub> nanoparticles was estimated to be 15.93nm from the Debye-Scherrer formula. The peaks at (100), (002), (101), (102), (110), (103), and (112) corresponded to standard hexagonal wurtzite ZnO (JCPDS card no. 36-1451), as shown in Figure 2b [14]. The average crystallite size of these ZnO nanoparticles was estimated to be 19.84 nm. Further, the composite showed crystalline phase peaks of both TiO<sub>2</sub> and ZnO, which confirmed the presence of both phases in the composite/heterostructure assembly (Fig. 2c) [27].

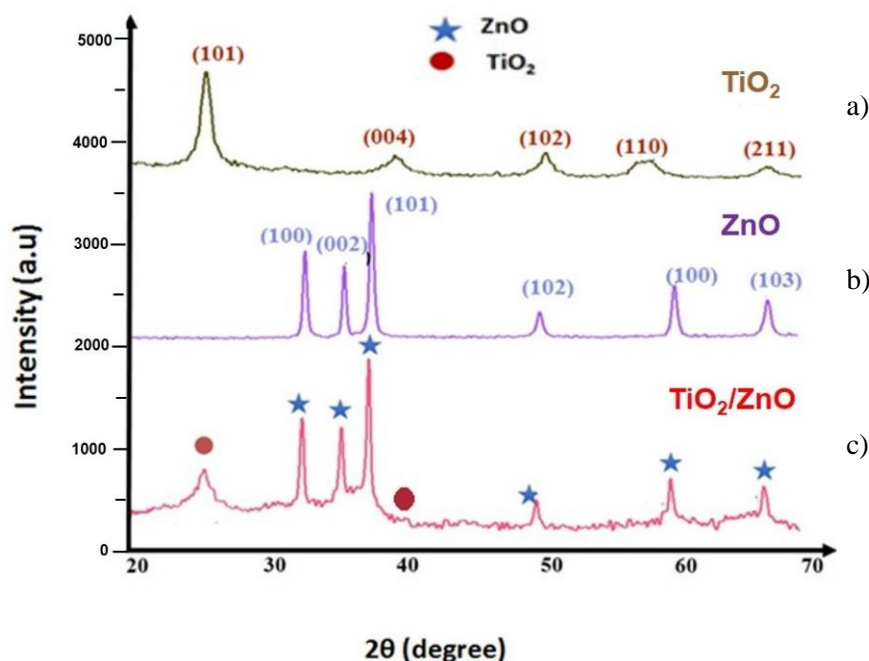


Fig. 2. XRD patterns of TiO<sub>2</sub>, ZnO and TiO<sub>2</sub>/ZnO nanocomposites

#### 3.2. Field emission scanning electron microscopy (FE-SEM) analysis

The morphological characteristics of synthesized samples were obtained from SEM. All the

catalyst samples, *i.e.* individual and composite assemblies (TiO<sub>2</sub>, ZnO, TiO<sub>2</sub>/ZnO), were made into a fine powder before taking SEM images. Figure 3a clearly shows the hexagonal shape of ZnO nanoparticles with less aggregation, whereas Fig. 3b

shows spherically shaped TiO<sub>2</sub> nanoparticles with little aggregation. Both the catalysts show good morphological structure due to prominent nucleation and crystal growth during synthesis, which was ascertained from sharp peaks observed from XRD analysis. However, the composite assembly,

TiO<sub>2</sub>/ZnO (Fig. 3c), shows aggregated particle assemblies consisting of both TiO<sub>2</sub> and ZnO nanoparticles with variations in size [27]. Further, the EDAX spectra taken for TiO<sub>2</sub> and ZnO samples confirm the presence of Ti, O and Zn in the electrode assemblies (Fig. S2, Supplementary Information).

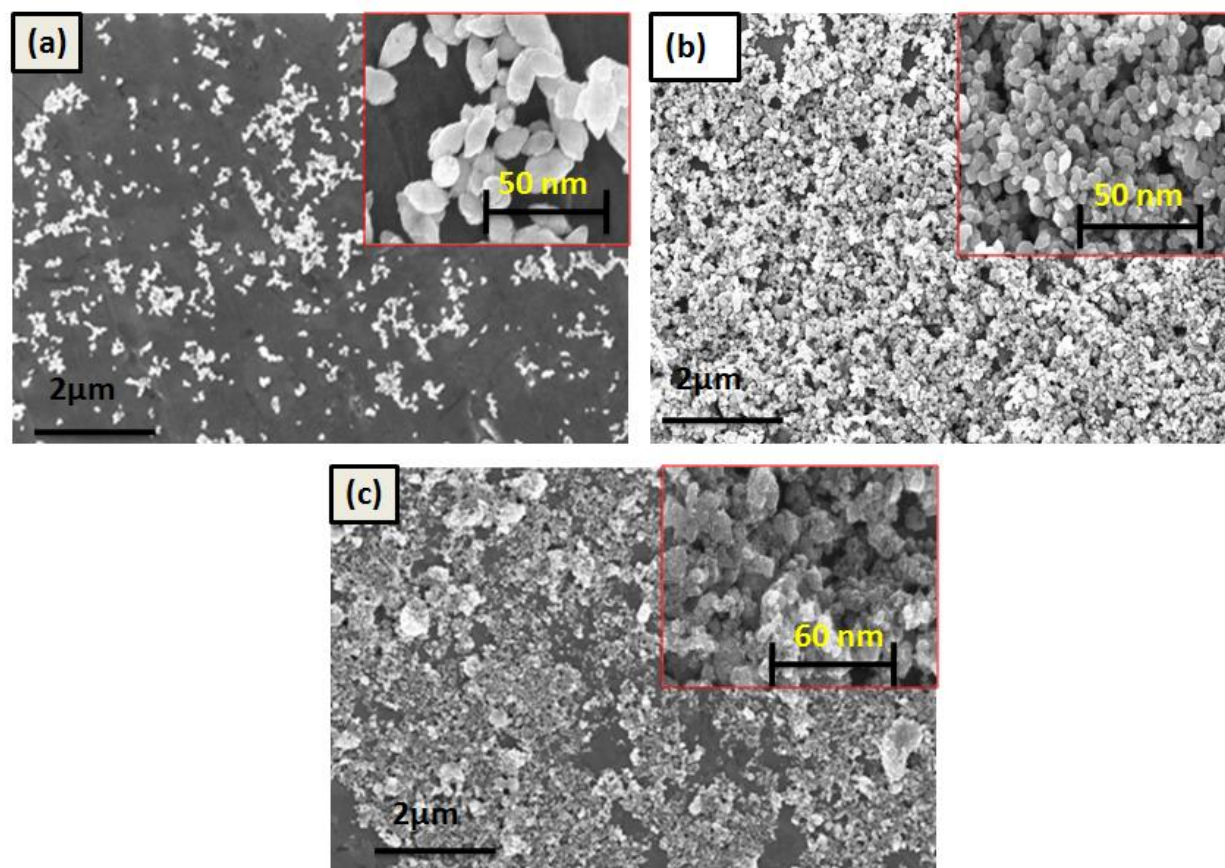


Fig. 3. Representative FE-SEM images of (a) ZnO, (b) TiO<sub>2</sub> and (c) TiO<sub>2</sub>/ZnO nanocomposite

### 3.3. FTIR analysis

FTIR analysis was performed to identify functional groups on the surface (Fig. 4). The broad peak observed at 3456 cm<sup>-1</sup> corresponds OH bending vibrations, whereas the peak at 612.49 cm<sup>-1</sup> indicates Zn–O stretching. The peaks at 1071, 1339, and 1557.95 cm<sup>-1</sup> were attributed to O–C–O asymmetric stretching vibrations [28]. The broad band observed at 3421 cm<sup>-1</sup> was assigned to the asymmetrical and symmetrical stretching vibrations of a hydroxyl group (–OH) of TiO<sub>2</sub>. The band at 1636.35 cm<sup>-1</sup> corresponded to deformative vibrations of Ti–OH stretching modes, and the band at 827.05 cm<sup>-1</sup> corresponded to the Ti–O bending mode of TiO<sub>2</sub>. Further, the presence of functional groups of both TiO<sub>2</sub> and ZnO moieties in compo-

site assembly confirmed heterostructure formation, as shown in Fig. 4.

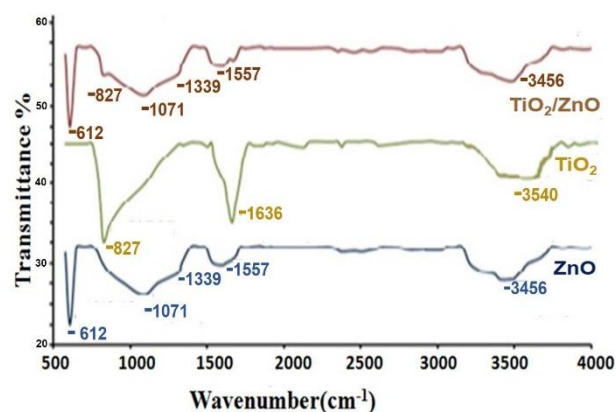


Fig. 4. FTIR spectra of ZnO, TiO<sub>2</sub>, and TiO<sub>2</sub>/ZnO nanocomposites

### 3.4. UV-Vis analysis

UV-Vis analysis (200–800 nm) was used to study the electrochemical degradation at various treatment times. The intense violet color of crystal violet shows an absorption band at  $\lambda_{\text{max}} = 576$  nm in the UV-Vis spectrum. The intensity of the peak at 576 nm decreased with an increase in treatment time (Fig. 5). The absorption at 576 nm became almost zero, as calculated from Eq. (1), with increasing treatment time with all electrodes, indicating the absence of auxochrome groups,  $-\text{N}(\text{CH}_3)$ ,

responsible for the color of the crystal violet dye [29, 30]. Electrochemical degradation before and during treatment (at various treatment times) was studied using UV-Vis analysis. Decolorization curves for bare Ti, Ti/TiO<sub>2</sub>, Ti/ZnO and Ti/TiO<sub>2</sub>/ZnO nanocomposites are shown in Figure 5 (a–d). The degradation times required to reach 80% decolorization for bare Ti, Ti/ZnO, Ti/TiO<sub>2</sub>, and Ti/TiO<sub>2</sub>/ZnO were 12, 10.5, 9 and 6.5 h, respectively, as shown in Table S1 (Supplementary information).

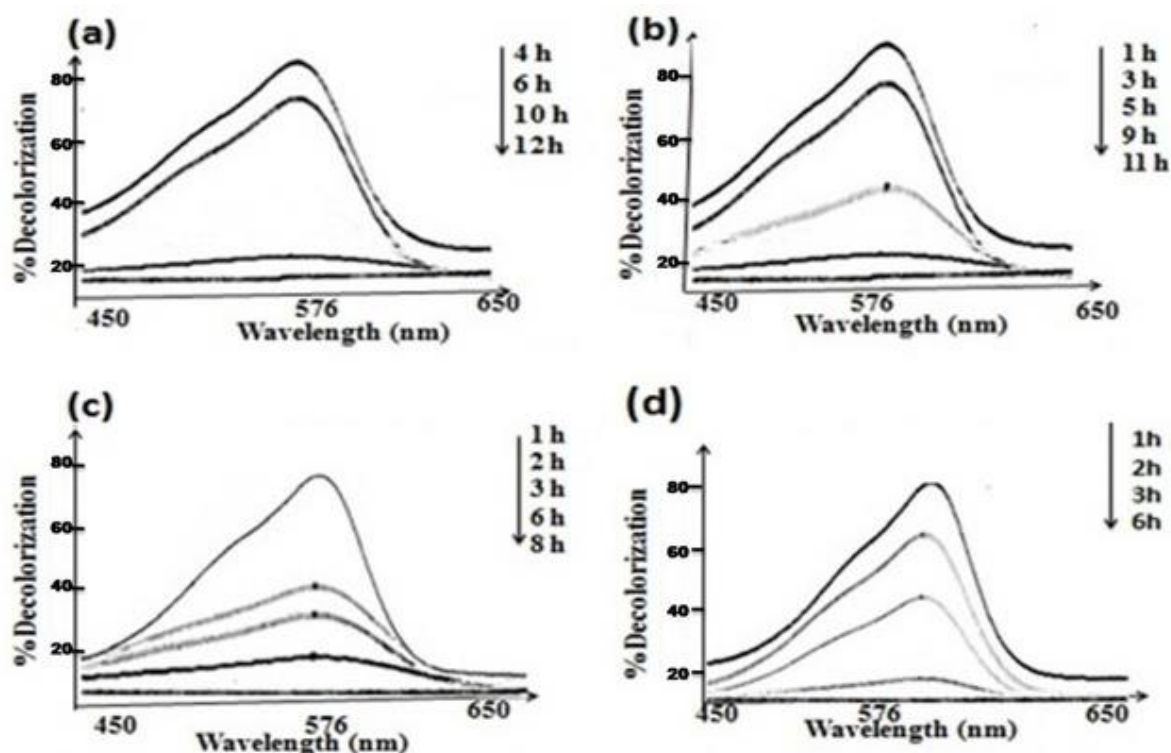
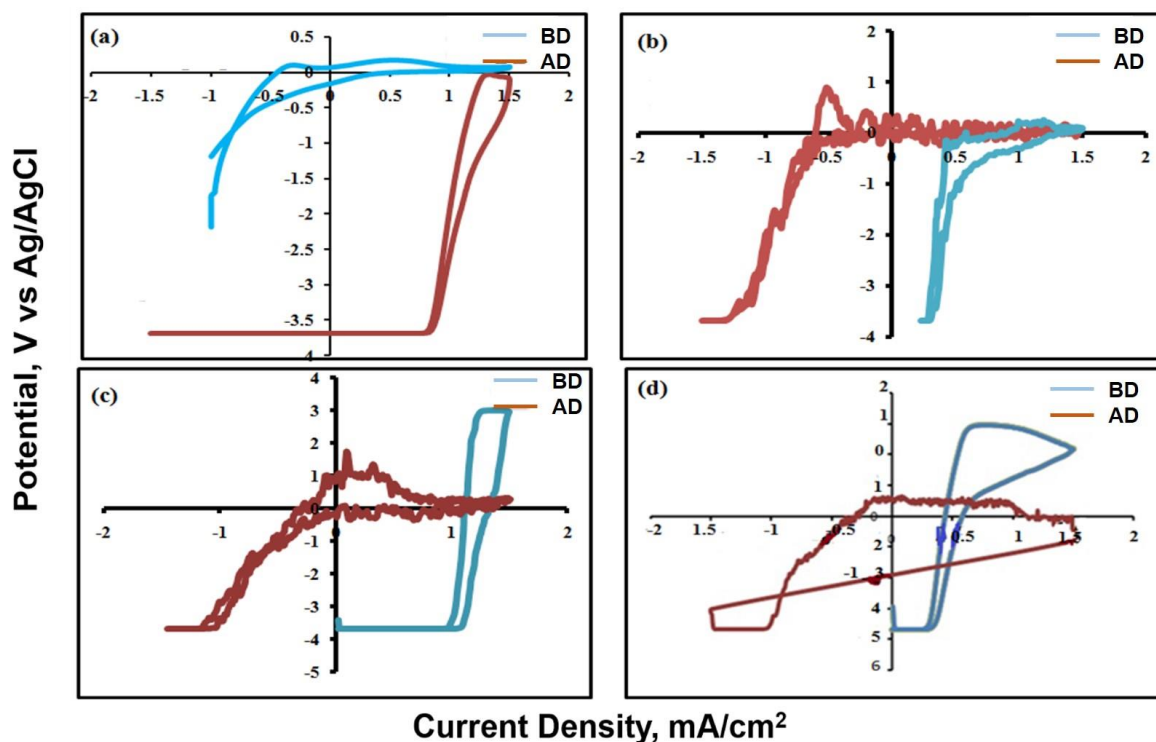


Fig. 5. Decolorization (%) vs. wavelength (nm) for (a) bare Ti, (b) Ti/TiO<sub>2</sub>, (c) Ti/ZnO and (d) Ti/TiO<sub>2</sub>/ZnO electrodes

### 3.5. CV studies

The amount of dye degradation was monitored with CV before and after electrochemical treatment (Fig. 6). Crystal violet degradation depends on electrolyte, as well as pH, as it is a bulky molecule of organic moieties, which can be cleaved upon supplement of electrical energy equivalent to dissociation energy [31]. During the forward CV scans, anodic peaks were observed at positive currents. Similarly, cathodic peaks were observed at negative currents during reverse CV scans. Decrease in anodic and cathodic peak cur-

rents were ascribed to the oxidation of reactive groups of crystal violet dye [31–33]. Before degradation, higher peak currents were due to the presence of more reactive groups in the dye, leading to higher oxidation of these groups. Then, after electrochemical treatment, the dye was completely decolorized, and hence, peak currents were decreased due to the absence of reactive groups (Fig. 6a–d). The best electrochemical performance was shown by the Ti/TiO<sub>2</sub>/ZnO nanocomposite assembly compared to the other fabricated electrodes (bare Ti, TiO<sub>2</sub>, ZnO).



**Fig. 6.** CV plots of crystal violet for dye degradation using (a) bare Ti, (b) Ti/TiO<sub>2</sub>, (c) Ti/ZnO, and (d) Ti/TiO<sub>2</sub>/ZnO, performed in 0.5M Na<sub>2</sub>SO<sub>4</sub> (three electrode measurements). AD and BD represent after degradation and before degradation, respectively.

### 3.6. Electrochemical dye degradation

The % decolorization vs. time plots for various electrode assemblies fabricated on Ti substrate are shown in Figure 7. Bare Ti substrate takes almost 12 h to reach nearly 80 % decolorization, whereas TiO<sub>2</sub> and ZnO assemblies fabricated on Ti substrate show more than 80 % decolorization in 10 and 12 h, respectively. The heterostructure assembly, TiO<sub>2</sub>/ZnO, shows better performance of nearly 85 % decolorization in 6.5 h.

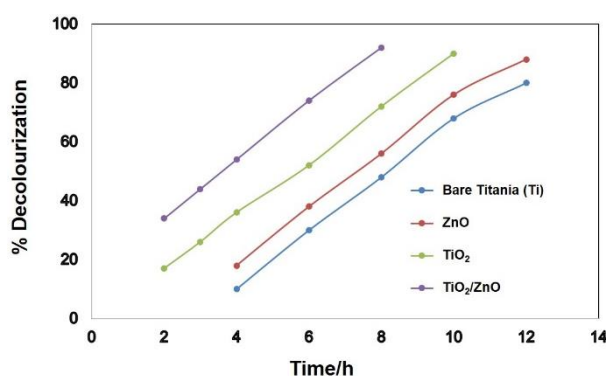


**Fig. 7.** Decolorization (%) vs. time for all fabricated electrode samples

This faster decolorization rate of the TiO<sub>2</sub>/ZnO nanocomposite electrode assembly is due to type-II

heterojunction formation with proper band edge alignments of TiO<sub>2</sub> and ZnO materials, which facilitates a fast charge carrier path across the interfaces.

### 3.7. Overall discussion

The increase in electrochemical performance of the composite electrode assembly compared with individual electrodes is likely due to the synergistic interaction, along with synchronized charge transport, helping to increase electrochemical activity (EC) [24]. Further, the formation of band edge alignments, through the type-II heterostructure of TiO<sub>2</sub>/ZnO nanocomposite, contributes a free path to electrons, enhancing the electronic conductivity and leading to quick oxygen evolution, as shown in Figure 8 [31]. Moreover, the large surface area of the nanocomposite assemblies accommodate more dye molecules to interact with oxidants, as shown in Fig. 8. Therefore, the TiO<sub>2</sub> and ZnO metal oxide heterostructure assembly achieves faster degradation compared to the individual metal oxides, and this behavior exemplifies the importance of heterostructure assemblies in dye degradation studies. Further, the detailed mechanism of crystal violet dye degradation and the degradation pathways were explained in our previous work [34, 35].

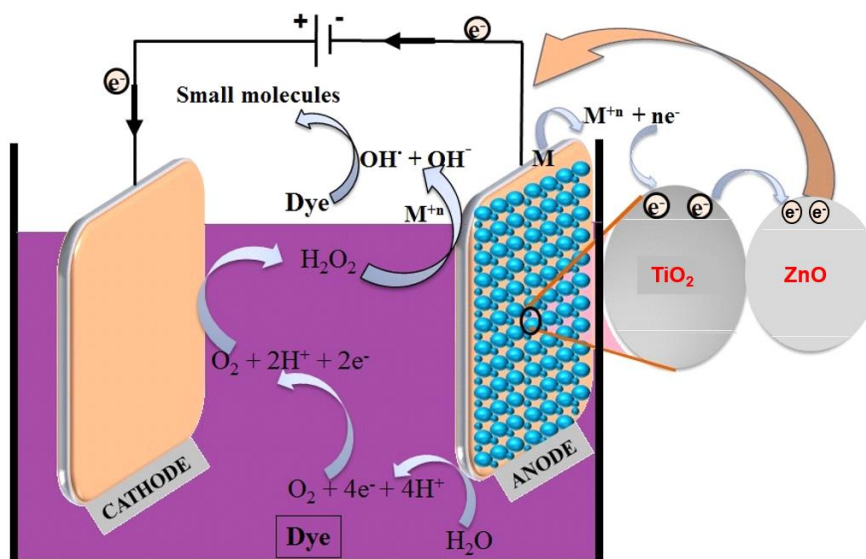


Fig. 8. TOC Graphic: Schematic representing the charge carrier path in electrochemical degradation

#### 4. CONCLUSIONS

The present study describes the importance of the type-II heterostructure assembly ( $\text{TiO}_2/\text{ZnO}$ ) fabricated on Ti substrate for electrochemical crystal violet dye degradation studies. Sol-gel synthesis was adopted for both pristine ( $\text{TiO}_2$ ,  $\text{ZnO}$ ) and composite assemblies ( $\text{TiO}_2/\text{ZnO}$ ). The synthesized electrode assemblies were characterized using XRD, SEM, UV-Vis, and FTIR analysis. The fabricated electrode assemblies on Ti substrate were tested for electrochemical analysis, and UV-Vis analysis was performed to understand crystal violet dye degradation. The heterostructured electro-catalyst assembly ( $\text{Ti}/\text{TiO}_2/\text{ZnO}$ ) showed enhanced performance over individual electro-catalytic assemblies, indicating faster electron transfer through the type-II heterostructure assembly due to synergistic interaction and synchronized charge transport across the material interfaces. Further, heterostructured electrode assemblies accommodate more oxidants and dye molecules, and hence, the rate of degradation was faster compared to individual electrode assemblies. The outcomes of the present study will not only help to design low-cost catalysts and associated heterostructure assemblies but also paves the path towards understanding the molecular mechanism of complex dye degradation studies.

**Acknowledgements.** We thank University Grants Commission (UGC), Govt. of India, for supporting this work through UGC XII plan funds, JNTUA, Anantapuramu.

**Disclosure statement.** No potential conflict of interest was reported by the authors

**Funding.** This work was supported by UGC, Govt. of India, under UGC XII plan funds, JNTUA, Anantapuramu.

#### REFERENCES

- [1] H. M. Pinheiro, E. Touraud, O. Thomas, Aromatic amines from azo dye reduction: status review with emphasis on direct UV spectrophotometric detection in textile industry wastewaters, *Dyes and pigments*, **61**, 121–139 (2004). DOI: doi.org/10.1016/j.dyepig.2003.10.009
- [2] G. S. Gupta, S. P. Shukla, G. Prasad, V. N. Singh, China clay as an adsorbent for dye house wastewaters, *Environ Technol*, **13**, 925–936 (1992). DOI: doi.org/10.1080/09593339209385228
- [3] R. A. Masoud, A. A., Haroun, N. H. El-Sayed, Dyeing of chrome tanned collagen modified by in situ grafting with 2-EHA and MAC, *J. Appl. Poly. Sci.*, **101**, 174–179 (2006). DOI: doi.org/10.1002/app.23160.
- [4] S. Komissarchik, &G. Nyanikova, Test systems and a method for express detection of synthetic food dyes in drinks, *LWT-Food Sci. Technol.*, **58**, 315–320 (2014). DOI:doi.org/10.1016/j.lwt.2014.03.038
- [5] R. W. Wagner, J. S. Lindsey, Boron-dipyromethane dyes for incorporation in synthetic multi-pigment light-harvesting arrays, *Pure Appl. Chem*, **68**, 1373–1380 (1996). DOI: doi.org/10.1351/pac199668071373
- [6] D. Wrobel, A. Boguta, R. M. Ion Mixtures of synthetic organic dyes in a photo-electronic cell, *J. Photochem. Photobiol., A Chem.*, **138**, 7–22 (2001). DOI: doi.org/10.1016/S1010-6030(00)00377-4
- [7] N. Daneshwar, H. A. Sorkhabi, M. Kobya, Decolorization of dye solution containing Acid Red 14 by electro-coagulation with a comparative investigation of different electrode connections, *J. Hazard. Mater*, **112**, 55–62 (2004). DOI: doi.org/10.1016/j.jhazmat.2004.03.021
- [8] A. Sakalis, D. Ansorgová, M. Holčápek, P. Jandera A. Voulgaropoulos, Analysis of sulphonated azodyes and their degradation products in aqueous solutions treated

- with a new electrochemical method, *Int. J. Environ. Anal. Chem.*, **84**, 875–888 (2004). DOI:doi.org/10.1080/03067310310001626731
- [9] J. S. Do, M. L. Chen, Decolourization of dye-containing solutions by electrocoagulation, *J. Appl. Electrochem.* **24**, 785–790 (1994). DOI: doi.org/10.1007/BF00578095
- [10] J. P. Lorimer, T. J. Mason, M. Plates, S. S. Phull, Dye effluent decolourisation using ultrasonically assisted electro-oxidation, *Ultrason. Sonochem.*, **7**, 237–242 (2000). DOI: doi.org/10.1016/S1350-4177(99)00045-0
- [11] H. Ma, B. Wang, X. Luo, Studies on degradation of methyl orange wastewater by combined electrochemical process, *J. Hazard. Mater.*, **149**, 492–498 (2007). DOI: doi.org/10.1016/j.jhazmat.2007.04.020
- [12] L. Fan, Y. Zhou, W. Yang, G. Chen, F. Yang, Electrochemical degradation of aqueous solution of Amaranth azo dye on ACF under potentiostatic model, *Dyes and Pigments*, **76**, 440–446 (2008). DOI: doi.org/10.1016/j.dyepig.2006.09.013
- [13] L. Szyrkowicz, C. Juzzolino, S. N. Kaul, S. Daniele, M. D. De Faveri, Electrochemical oxidation of dyeing baths bearing disperse dyes, *Ind. Eng. Chem. Res.*, **39**, 3241–3248 (2000). DOI: doi.org/10.1021/ie9908480
- [14] M. A. Sanroman, M. Pazos, M. T. Ricart, C. Cameselle, Electrochemical decolourisation of structurally different dyes, *Chemosphere*, **57**, 233–239 (2004). DOI: doi.org/10.1016/j.chemosphere.2004.06.019
- [15] M. Murati, N. Oturan, Z. Zdravkovski, J. P. Stanoeva, S. E. Aaron, J. J. Aaron, M. A. Oturan, Application of the electro-Fenton process to mesotrione aqueous solutions: Kinetics, degradation pathways, mineralization and evolution of the toxicity, *Maced. J. Chem. Chem. Eng.*, **33**, 121–137 (2014).
- [16] A. Fernandes, A. Morao, M. Magrinho, A. Lopes, I. Gonçalves, Electrochemical degradation of CI acid orange 7, *Dyes and Pigments*, **61**, 287–296 (2004). DOI: doi.org/10.1016/j.dyepig.2003.11.008
- [17] R. Saravanan, F. Gracia Mohammad, Mansoob Khan, V. Poornima, Vinod Kumar Gupta, V. Narayanan, A. Stephen, ZnO/CdO nanocomposites for textile effluent degradation and electrochemical detection, *J. Mol. Liq.*, **209**, 374–380 (2015). DOI: doi.org/10.1016/j.molliq.2015.05.040
- [18] Lin Yue, Kaihong Wang, Jianbo Guo, Jingliang Yang, Xiao Luo, Jing Lian, Li Wang, Enhanced electrochemical oxidation of dye wastewater with Fe<sub>2</sub>O<sub>3</sub> supported catalyst, *J. Ind. Eng. Chem.* **20**, 725–731 (2014). DOI: doi.org/10.1016/j.jiec.2013.06.001
- [19] Z. M. Shen, D. Wu, J. Yang, T. Yuan, W. H. Wang, J. P. Jia, Methods to improve electrochemical treatment effect of dye wastewater, *J. Haz. Mat.*, **131**, 90–97 (2006). DOI: doi.org/10.1016/j.jhazmat.2005.09.010
- [20] S. Rajendran, M. Mansoob Khan, F. Gracia, Jiaqian Qin, Vinod Kumar Gupta, Stephen Arumainathan, Ce<sup>+3</sup> ion induced visible light photocatalytic degradation and electrochemical activity of ZnO/CeO<sub>2</sub> nanocomposite, *Sci. Rep.*, **6**, 31641 (2016). DOI:doi.org/10.1038/srep31641
- [21] R. Pelegrini, P. Peralta-Zamora, A. R. de Andrade, J. Reyes, N. Durán, Electrochemically assisted photocatalytic degradation of reactive dyes. *App. Catal. B: Envi.* **22**, 83–90 (1999). DOI:doi.org/10.1016/S0926-3373(99)00037-5
- [22] Astam K. Patra, Arghya Dutta, Asim Bhaumik, Highly ordered mesoporous TiO<sub>2</sub>-Fe<sub>2</sub>O<sub>3</sub> mixed oxide synthesized by sol-gel pathway: an efficient and reusable heterogeneous catalyst for dehalogenation reaction, *ACS Appl. Mater. Interfaces*, **4**, 5022–5028 (2012). DOI: doi.org/10.1021/am301394u
- [23] T. Jagadale, M. Kulkarni, D. Pravarthana, W. Ramadan, P. Thakur, Photocatalytic degradation of azo dyes using Au: TiO<sub>2</sub>, γ-Fe<sub>2</sub>O<sub>3</sub>: TiO<sub>2</sub> functional nanosystems. *J. Nanosci. Nanotechnol.*, **12**, 928–936 (2012). DOI: 10.1166/jnn.2012.5171
- [24] Dilip Kumar Behara, Ashok Kumar Ummireddi, Vidyasagar Aragonda, Prashant Kumar Gupta, Raj Ganesh S. Pala and Sri Sivakumar, Coupled optical absorption, charge carrier separation, and surface electrochemistry in surface disordered/hydrogenated TiO<sub>2</sub> for enhanced PEC water splitting reaction, *Phys. Chem. Chem. Phys.*, **18**, 8364–8377 (2016). DOI: doi.org/10.1039/C5CP04212G
- [25] A. K. Singh, Synthesis, characterization, electrical and sensing properties of ZnO nanoparticles, *Adv. Powder Tech.*, **21**, 609–613 (2010). DOI: doi.org/10.1016/j.apt.2010.02.002
- [26] J. Tian, L. Chen, J. Dai, X. Wang, Y. Yin, P. Wu, Preparation and characterization of TiO<sub>2</sub>, ZnO and TiO<sub>2</sub>/ZnO nanofilms via sol-gel process, *Cer. Int.*, **35**, 2261–2270 (2009). DOI: doi.org/10.1016/j.ceramint.2008.12.010
- [27] M. A. Habib, M. T. Shahadat, N. M. Bahadur, I. M. Ismail, A. J. Mahmood, Synthesis and characterization of ZnO-TiO<sub>2</sub> nanocomposites and their application as photocatalysts, *Int. Nano Lett.*, **3**, 5 (2013). DOI:doi.org/10.1186/2228-5326-3-5
- [28] R. Sharma, F. Alam, A. K. Sharma, V. Dutta, S. K. Dhawan, ZnO anchored graphene hydrophobic nanocomposite-based bulk heterojunction solar cells showing enhanced short-circuit current, *J. Mat. Chem. C*, **2**, 8142–8151 (2014). DOI: doi.org/10.1039/C4TC01056F
- [29] Seema Singh, Vimal Chandra Srivastava, Indra Deo Mall, Mechanism of dye degradation during electrochemical treatment, *J. Phys. Chem. C*, **117**, 15229–15240 (2013). DOI:doi.org/10.1021/jp405289f
- [30] H. J. Fan, S. T. Huang, W. H. Chung, J. L. Jan, W. Y. Lin, C. C. Chen, Degradation pathways of crystal violet by Fenton and Fenton-like systems: condition optimization and intermediate separation and identification, *J. Haz. Mat.*, **171**, 1032–1044 (2009). DOI: doi.org/10.1016/j.jhazmat.2009.06.117
- [31] V. V. Perekotii, Z. A. Temerdashev, T. G. Tsyupko, E. A. Palenaya, Electrochemical behavior of crystal violet on glassy carbon electrodes, *J. Anal. Chem.*, **57**, 5, 448–451 (2002). DOI: https://doi.org/10.1023/A:1015421927771
- [32] Milica Jović, Dalibor Stanković, Dragan Manojlović, Ivan Anđelković, Anđelija Milić, Biljana Dojčinović, Goran Roglić, Study of the electrochemical oxidation of reactive textile dyes using platinum electrode. *Int. J. Electrochem. Sci.*, **8**, 168–183 (2013).

- [33] A. A. Peláez-Cid, S. Blasco-Sancho, F. M. Matysik, Determination of textile dyes by means of non-aqueous capillary electrophoresis with electrochemical detection. *Talanta*, **75**, 5, 1362–1368 (2008). DOI:<https://doi.org/10.1016/j.talanta.2008.01.049>
- [34] P. S. Palukuru, V. Devangam A., D. K. Behara, N, S-codoped TiO<sub>2</sub>/Fe<sub>2</sub>O<sub>3</sub> heterostructure assemblies for electrochemical degradation of crystal violet dye, *Iran. J. Chem. Chem.*, **39**, 171–180, (2020). DOI:10.30492/IJCCE.2020.33368
- [35] D. K. Behara, S. M. Mukkara, T. Jalajakshi, TiO<sub>2</sub>/Fe<sub>2</sub>O<sub>3</sub>: Type-I heterostructures for electrochemical dye degradation/water splitting studies, *J. Inst. Eng. India Ser. E*, **100**, 189–198 (2019). DOI:[doi.org/10.1007/s40034-019-00148-y](https://doi.org/10.1007/s40034-019-00148-y).